# Translational motion of two interacting bubbles in a strong acoustic field

Alexander A. Doinikov
*Institute of Nuclear Problems, Byelorussian State University, 11 Bobruiskaya Street, Minsk 220050, Belarus*
(Received 20 February 2001; published 16 July 2001)

Using the Lagrangian formalism, equations of radial and translational motions of two coupled spherical gas bubbles have been derived up to terms of third order in the inverse distance between the bubbles. The equations of radial pulsations were then modified, for the purpose of allowing for effects of liquid compressibility, using Keller-Miksis' approach, and the equations of translation were added by viscous forces in the form of the Levich drag. This model was then used in a numerical investigation of the translational motion of two small, driven well below resonance, bubbles in strong acoustic fields with pressure amplitudes exceeding 1 bar. It has been found that, if the forcing is strong enough, the bubbles form a bound pair with a steady spacing rather than collide and coalesce, as classical Bjerknes theory predicts. Moreover, the viscous forces cause skewness in the system, which results in self-propulsion of the bubble pair. The latter travels as a unit along the center line in a direction that is determined by the ratio of the initial bubble radii. The results obtained are of immediate interest for understanding and modeling collective bubble phenomena in strong fields, such as acoustic cavitation streamers.

DOI: 10.1103/PhysRevE.64.026301 PACS number(s): 47.55.Bx, 47.55.Dz, 47.55.Kf, 43.25.+y

## I. INTRODUCTION

According to classical Bjerknes theory [1], if two bubbles are driven below or above their natural (Minnaert) frequencies, they attract each other, whereas if the driving frequency is in between the two natural frequencies, the bubbles repel each other. However, experiments show that even in a weak acoustic field, bubble dynamics does not necessarily follow this scenario. For instance, it was observed more than once [2,3] that bubbles, driven above resonance, formed stable clusters with persistent separation distances comparable to the bubble size, which were given the name ''bubble grapes.'' In a strong field, bubbles exhibit even more intricate behavior: They group themselves into branched filamentary structures that are referred to as acoustic streamers [4]. Unlike the bubble grapes, the streamers are composed of small cavitation bubbles that are driven well below resonance. Physical mechanisms responsible for the bubble grapes are now clear enough [5], but this is not true for the cavitation streamers. Mettin *et al.* [6] have investigated numerically the time-averaged interaction force between two small bubbles in strong sound fields with pressure amplitudes exceeding 1 bar. For calculation of the bubble oscillations, they used the Keller-Miksis model [7] which was supplemented with terms allowing for radiation coupling between the bubbles. It was found that, for some bubble pairs, where one bubble was a little smaller and the other bubble larger than the resonance size corresponding to the dynamical Blake threshold, the interaction force could change from attraction to repulsion as the bubbles came close to each other, although the driving frequency was always much smaller than the linear resonance frequencies of the two bubbles. This implies the existence of a stable equilibrium distance between two strongly oscillating bubbles. However, as the authors themselves conclude, their findings cannot explain the structure of acoustic streamers because of the predominant attractive situations in parameter space.

The present paper proposes a model that makes possible a direct calculation of the translational motion (instead of the mean forces as in [6]) of two interacting spherical gas bubbles in a strong acoustic field. The model includes four combined ordinary differential equations of second order that describe the coupled volume and translational oscillations of the bubbles and take account of viscous drag forces on them. The application of this model to the parameter space characteristic of acoustic streamers reveals that for most combinations of bubble radii, contrary to the predictions of [6], a mutual approach results in a dynamically equilibrium separation distance between the bubbles rather than collision and coalescence. It is apparent that this result can provide an explanation for the structure of acoustic streamers.

## II. MATHEMATICAL MODEL

Consider two gas bubbles, undergoing volume and translational oscillations, in a perfect incompressible liquid. Suppose that the spacing between the bubbles is large compared with their size so that the bubbles remain spherical at all times. Using local spherical coordinates originated at the moving centers of the bubbles (Fig. 1), the boundary conditions at the bubble surfaces can be represented as

$$\frac{\partial \varphi}{\partial r_j} = \dot{R}_j + \dot{x}_j \cos\theta_j \quad \text{at} \quad r_j = R_j(t), \quad j = 1,2, \tag{1}$$

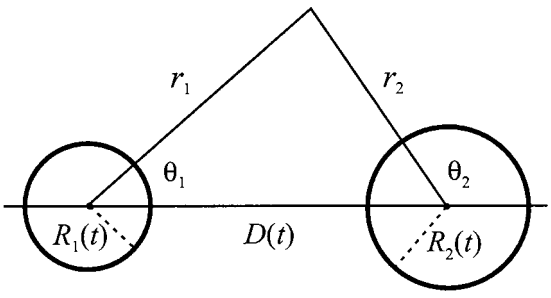


FIG. 1. Geometry of the system.

 

where $\varphi$ is the velocity potential, $R_j(t)$ and $x_j(t)$ are the time-dependent radius and position of the center of the $j$th bubble, respectively, and the overdot denotes the time derivative. The velocity potential, satisfying the Laplace equation $\Delta\varphi=0$, can be expanded as

$$\varphi=\varphi_1+\varphi_2, \tag{2}$$

where $\varphi_j$, the scattered potential of the $j$th bubble, is given by

$$\varphi_j=\sum_{n=0}^{\infty} A_n^{(j)}(t) r_j^{-n-1} P_n(\mu_j), \tag{3}$$

$$=\sum_{n=0}^{\infty} B_n^{(j)}(t) r_{3-j}^{n} P_n(\mu_{3-j}). \tag{4}$$

Here $\mu_j=\cos\theta_j$ and $P_n$ is the Legendre polynomial. Equation (3) gives $\varphi_j$ in the proper coordinates of the $j$th bubble and Eq. (4) in the coordinates of the other bubble, $j=1\rightarrow 3-j=2$, and vice versa. [Note also that Eq. (4) is only valid in the vicinity of the second bubble, which is quite enough to gain our ends, though.] A relation between $A_n^{(j)}$ and $B_n^{(j)}$ is obtained using the well-known identity [8]

$$\frac{P_n(\mu_j)}{r_j^{n+1}}=\frac{(-1)^{n(j-1)}}{D^{n+1}}\sum_{m=0}^{\infty}\frac{(-1)^{jm}(n+m)!}{n!m!}\times\left(\frac{r_{3-j}}{D}\right)^m P_m(\mu_{3-j}), \tag{5}$$

where $D(t)$ is the time-dependent distance between the translating centers of the bubbles. The result is as follows:

$$B_n^{(j)}(t)=\frac{(-1)^{jn}}{D^{n+1}}\sum_{m=0}^{\infty}\frac{(-1)^{(j-1)m}(n+m)!}{n!m!D^m}A_n^{(j)}(t). \tag{6}$$

Then, utilizing Eqs. (3) and (4), the total velocity potential near the $j$th bubble is written as

$$\varphi=\sum_{n=0}^{\infty}[A_n^{(j)}(t)r_j^{-n-1}+B_n^{(3-j)}(t)r_j^n]P_n(\mu_j). \tag{7}$$

Substitution of this equation into the boundary conditions, Eq. (1), yields

$$A_0^{(j)}=-\dot{R}_jR_j^2,\quad A_n^{(j)}=-\frac{\dot{x}_jR_j^3}{2}\delta_{n1}+\frac{nR_j^{2n+1}}{n+1}B_n^{(3-j)} \quad \text{for } n\geqslant 1. \tag{8}$$

Here $\delta_{nm}$ is the Kronecker delta and the time dependence is omitted for the sake of simplicity. It is easy to see that Eqs. (6) and (8) allow us to get the coefficients $A_n^{(j)}$ and $B_n^{(j)}$ with any required accuracy with respect to the small parameters $R_j/D$.

The next step is the construction of the Lagrangian function of the system $L=T-U$. The kinetic energy $T$ of the system is determined by the kinetic energy of the host liquid,

$$T=\frac{\rho}{2}\int|\nabla\varphi|^2dV, \tag{9}$$

with $\rho$ denoting the liquid density and $V$ the volume occupied by the liquid. The potential energy $U$ of the system can be represented as

$$U=-p_1V_1-p_2V_2-x_1F_{ex1}-x_2F_{ex2}, \tag{10}$$

where $p_j$ is the scattered pressure at the surface of the $j$th bubble, $V_j=4\pi R_j^3/3$ is the time-varying volume of the $j$th bubble, and $F_{exj}$ denotes an external force on the $j$th bubble, such as viscous drag. Equation (9) can be transformed to the sum $T=T_1+T_2$ with

$$T_j=-\pi\rho R_j^2\int_{-1}^{1}\left(\varphi\frac{\partial\varphi}{\partial r_j}\right)_{r_j=R_j}d\mu_j. \tag{11}$$

On substitution of Eqs. (1) and (7), Eq. (11) gives

$$T_j=2\pi\rho\left(R_j^3\dot{R}_j^2-\frac{1}{3}R_j^3\dot{x}_j^2-R_j^2\dot{R}_jB_0^{(3-j)}-\dot{x}_jA_1^{(j)}\right). \tag{12}$$

Further calculation will be carried out with accuracy up to terms of third order in $D^{-1}$. From Eqs. (6) and (8), one obtains

$$A_1^{(j)}\approx-\frac{R_j^3}{2}\left(\dot{x}_j-\frac{(-1)^jR_{3-j}^2\dot{R}_{3-j}}{D^2}-\frac{R_{3-j}^3\dot{x}_{3-j}}{D^3}\right), \tag{13}$$

$$B_0^{3-j}\approx-\frac{R_{3-j}^2}{2D}\left(2\dot{R}_{3-j}+\frac{(-1)^jR_{3-j}\dot{x}_{3-j}}{D}\right)+O(D^{-4}). \tag{14}$$

Substituting Eqs. (13) and (14) into Eq. (12) and using Eq. (10), one finds the Lagrangian function of the system as

$$L=2\pi\rho\left[R_1^3\dot{R}_1^2+R_2^3\dot{R}_2^2+\frac{R_1^3\dot{x}_1^2}{6}+\frac{R_2^3\dot{x}_2^2}{6}+\frac{2R_1^2R_2^2\dot{R}_1\dot{R}_2}{D}+\frac{R_1^2R_2^2(R_1\dot{R}_2\dot{x}_1-R_2\dot{R}_1\dot{x}_2)}{D^2}-\frac{R_1^3R_2^3\dot{x}_1\dot{x}_2}{D^3}\right]+\frac{4\pi}{3}(p_1R_1^3+p_2R_2^3)+x_1F_{ex1}+x_2F_{ex2}. \tag{15}$$

Considering $R_j$, $x_j$, $\dot{R}_j$, and $\dot{x}_j$ as generalized coordinates and velocities, the equations of radial and translational motions of the bubbles are obtained in the usual way through the use of the Lagrangian equations

$$\frac{d}{dt}\frac{\partial L}{\partial\dot{q}_i}-\frac{\partial L}{\partial q_i}=0. \tag{16}$$

This yields four combined ordinary differential equations of second order:

$$R_1\ddot{R}_1+\frac{3}{2}\dot{R}_1^2-\frac{p_1}{\rho}=\frac{\dot{x}_1^2}{4}-\frac{R_2^2\ddot{R}_2+2R_2\dot{R}_2^2}{D}+\frac{R_2^2(\dot{x}_1\dot{R}_2+R_2\ddot{x}_2+5\dot{R}_2\dot{x}_2)}{2D^2}-\frac{R_2^3\dot{x}_2(\dot{x}_1+2\dot{x}_2)}{2D^3}, \tag{17}$$

$$R_2\ddot{R}_2+\frac{3}{2}\dot{R}_2^2-\frac{p_2}{\rho}=\frac{\dot{x}_2^2}{4}-\frac{R_1^2\ddot{R}_1+2R_1\dot{R}_1^2}{D}-\frac{R_1^2(\dot{x}_2\dot{R}_1+R_1\ddot{x}_1+5\dot{R}_1\dot{x}_1)}{2D^2}-\frac{R_1^3\dot{x}_1(\dot{x}_2+2\dot{x}_1)}{2D^3}, \tag{18}$$

$$\frac{R_1\ddot{x}_1}{3}+\dot{R}_1\dot{x}_1+\frac{1}{D^2}\frac{d}{dt}(R_1R_2^2\dot{R}_2)-\frac{R_2^2(R_1R_2\ddot{x}_2+R_2\dot{R}_1\dot{x}_2+5R_1\dot{R}_2\dot{x}_2)}{D^3}=\frac{F_{ex1}}{2\pi\rho R_1^2}, \tag{19}$$

$$\frac{R_2\ddot{x}_2}{3}+\dot{R}_2\dot{x}_2-\frac{1}{D^2}\frac{d}{dt}(R_2R_1^2\dot{R}_1)-\frac{R_1^2(R_1R_2\ddot{x}_1+R_1\dot{R}_2\dot{x}_1+5R_2\dot{R}_1\dot{x}_1)}{D^3}=\frac{F_{ex2}}{2\pi\rho R_2^2}. \tag{20}$$

Equations (17) and (18) govern radial pulsations of the bubbles and Eqs. (19) and (20) their translation. Assuming that the bubbles are driven by the acoustic pressure field $P_{ex}(t)=-P_a\sin\omega t$, the pressure $p_j$ is taken in the form

$$p_j=\left(P_0+\frac{2\sigma}{R_{j0}}\right)\left(\frac{R_{j0}}{R_j}\right)^{3\gamma}-\frac{2\sigma}{R_j}-\frac{4\eta\dot{R}_j}{R_j}-P_0+P_a\sin\omega t, \tag{21}$$

where $R_{j0}$ is the equilibrium radius of the $j$th bubble, $P_0$ is the hydrostatic pressure, $\sigma$ is the surface tension, $\gamma$ is the polytropic exponent of the gas within the bubbles, and $\eta$ is the viscosity of the liquid. The external forces $F_{exj}$ are set equal to the Levich viscous drag [9]:

$$F_{exj}=-12\pi\eta R_j(\dot{x}_j-v_{3-j}), \tag{22}$$

where $v_j$ denotes the liquid velocity that is generated by the $j$th bubble at the center of the other bubble. Up to order $D^{-3}$, this velocity is given by

$$v_j=-\frac{(-1)^jR_j^2\dot{R}_j}{D^2}+\frac{R_j^3\dot{x}_j}{D^3}. \tag{23}$$

The left-hand sides of Eqs. (17) and (18) are simply the Rayleigh-Plesset equations. Terms due to translational motion and bubble coupling are grouped on the right-hand sides. It is known that for large forcing amplitudes the Rayleigh-Plesset equation yields unsatisfactory results since the velocity of radial oscillations is no longer small compared with the sound speed in the liquid. Better results are provided by the Keller-Miksis model [7], which allows for acoustic radiation from bubbles. To make Eqs. (17) and (18) adequate for large forcing amplitudes, we can just replace their left-hand sides with the Keller-Miksis equations, keeping the right-hand sides intact. This results in

$$\left(1-\frac{\dot{R}_1}{c}\right)R_1\ddot{R}_1+\left(\frac{3}{2}-\frac{\dot{R}_1}{2c}\right)\dot{R}_1^2-\frac{1}{\rho}\left(1+\frac{\dot{R}_1}{c}\right)p_1-\frac{R_1}{\rho c}\frac{dp_1}{dt}=\frac{\dot{x}_1^2}{4}-\frac{R_2^2\ddot{R}_2+2R_2\dot{R}_2^2}{D}+\frac{R_2^2(\dot{x}_1\dot{R}_2+R_2\ddot{x}_2+5\dot{R}_2\dot{x}_2)}{2D^2}-\frac{R_2^3\dot{x}_2(\dot{x}_1+2\dot{x}_2)}{2D^3}, \tag{24}$$

$$\left(1-\frac{\dot{R}_2}{c}\right)R_2\ddot{R}_2+\left(\frac{3}{2}-\frac{\dot{R}_2}{2c}\right)\dot{R}_2^2-\frac{1}{\rho}\left(1+\frac{\dot{R}_2}{c}\right)p_2-\frac{R_2}{\rho c}\frac{dp_2}{dt}=\frac{\dot{x}_2^2}{4}-\frac{R_1^2\ddot{R}_1+2R_1\dot{R}_1^2}{D}-\frac{R_1^2(\dot{x}_2\dot{R}_1+R_1\ddot{x}_1+5\dot{R}_1\dot{x}_1)}{2D^2}-\frac{R_1^3\dot{x}_1(\dot{x}_2+2\dot{x}_1)}{2D^3}, \tag{25}$$

where $c$ is the speed of sound in the liquid. The translational equations, Eqs. (19) and (20), can also be left untouched since in most cases of interest the translational velocities of the bubbles are small compared with their radial velocities.

## III. NUMERICAL RESULTS

Calculations have been made for two air bubbles in water at the driving frequency $f=20$ kHz. The other parameters were set to $P_0=1$ bar, $\rho=998$ kg/m$^3$, $\sigma=0.0725$ N/m, $\eta=0.001$ kg/(m s), $c=1500$ m/s, and $\gamma=1.4$. The system of equations (19), (20), (24), and (25) was solved using the program MATHEMATICA. The results obtained are presented in Figs. 2–4.

Figure 2 shows trajectories of various bubble pairs. The choice of the equilibrium bubble radii was motivated by the presumed bubble size distribution in acoustic streamers [6], according to which the majority of the cavitating bubbles has an equilibrium radius below 10 $\mu$m. The trajectories are formed by the positions of the bubble centers at the end of each acoustic cycle; i.e., they are smoothed rather than real bubble paths. Examples of real bubble paths for the initial stage of motion are given in Fig. 3. The lower curves of Figs.

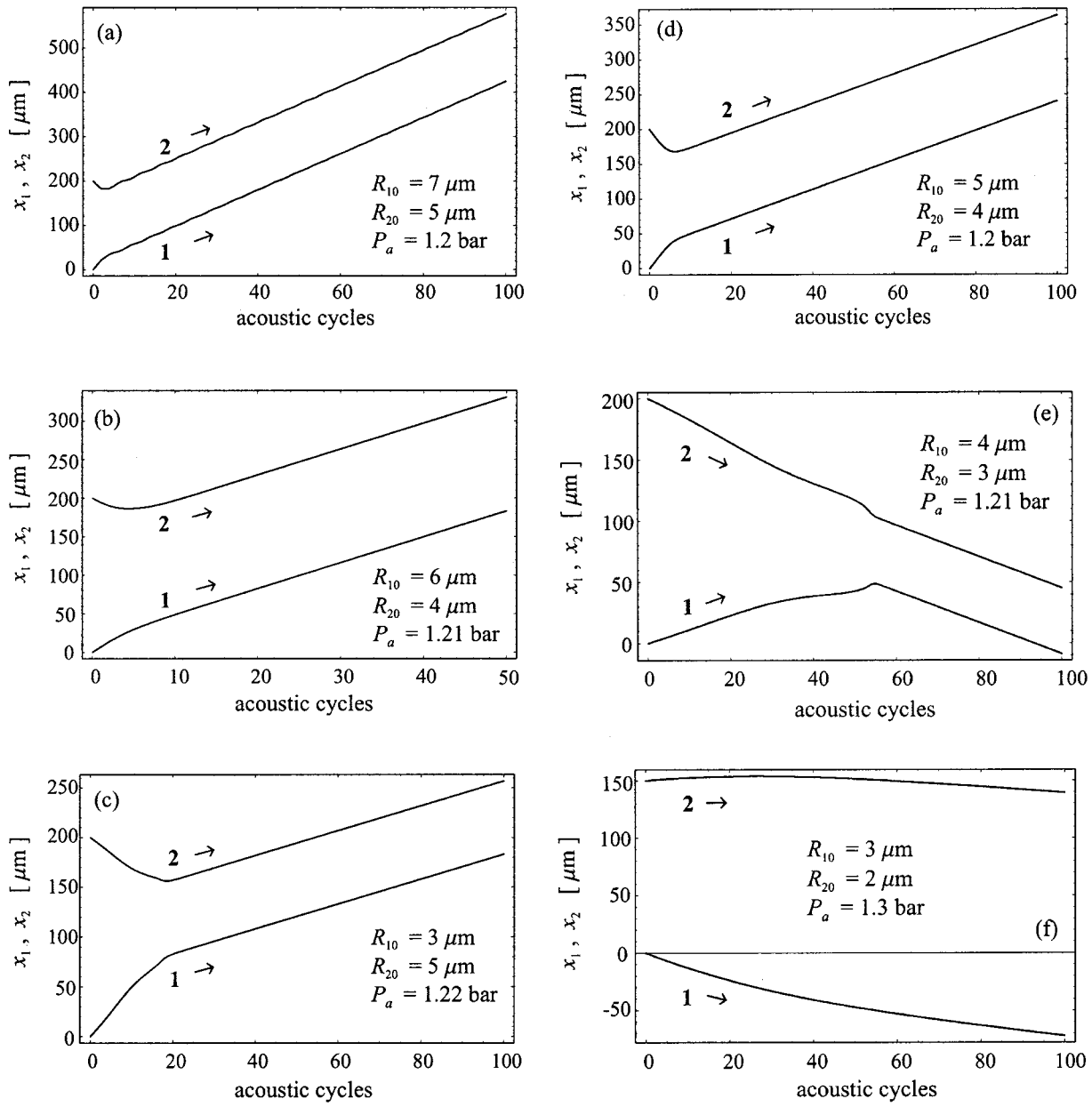


FIG. 2. Smoothed paths of bubble pairs. The positions of the bubbles are taken at the end of each acoustic cycle.

2 and 3 correspond to bubble 1 and the upper curves to bubble 2. It is seen that, although the bubble radii of the examined pairs are varied over a fairly wide range, the mutual approach of the bubbles results in a dynamical equilibrium separation distance rather than collision and coalescence. Contact of bubbles was observed only if their radii were sufficiently close. Situations of this sort are illustrated by Fig. 4(a), where the upper curve is the time-varying distance between the moving bubble centers, $D(t)$, and the lower curve is the sum of the instantaneous bubble radii, $R_1(t)+R_2(t)$. It is seen that the bubbles come into contact in 7.5 acoustic cycles. For comparison, Fig. 4(b) shows a similar plot for one of the noncolliding bubble pairs of Fig. 2. Contact also occurs if the forcing is set weak. For instance, the bubble pair shown in Fig. 4(b) comes into contact in 95 acoustic cycles for initial separation distance $D(0)$ $=30\ \mu$m when the driving pressure $P_a$ is set to 0.9 bar. Besides, it is found that in all cases investigated the bubbles collide very quickly if the viscous forces are omitted from the equations.

So the fact that the bubble pairs shown in Fig. 2 are prevented from coalescing can most likely be explained by a combined effect of high-amplitude bubble pulsations and viscous forces. Every acoustic cycle, the attractive secondary Bjerknes force attempts to bring the bubbles together. But each of the bubbles generates a very strong velocity field in the surrounding liquid, the intensity of which increases rapidly as the spacing between the bubbles decreases. The velocity fields give rise to vigorous viscous drag forces, which decelerate the bubbles and, owing to inertia, cause them to turn back. These attempts of alternate approaches and rebounds can be easily seen in Fig. 3. As a result, a dynamical

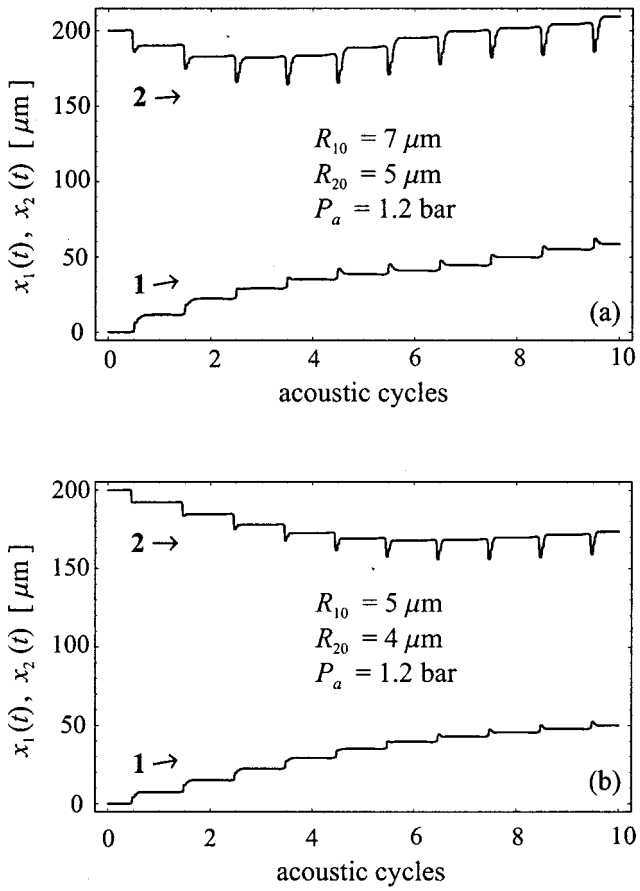


FIG. 3. Examples of real bubble paths.

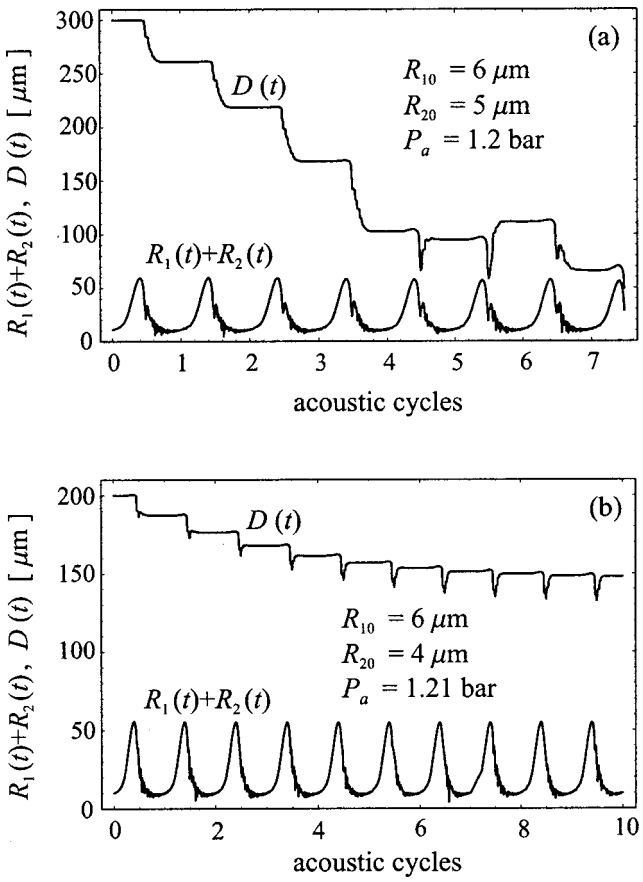


FIG. 4. The sum of the instantaneous bubble radii $R_1(t)+R_2(t)$ and the time-varying distance between the bubble centers $D(t)$ as functions of the number of acoustic cycles for (a) colliding and (b) noncolliding bubble pairs.

steady state is established at which the distance between the bubbles remains, on average, constant. Obviously this result can provide an explanation of why, instead of coalescing as Bjerknes theory requires, cavitation bubbles in acoustic streamers form a line at stable intervals.

Another interesting effect that follows from Fig. 2 is that the bubble pairs undergo self-propulsion. In Figs. 2(a), 2(b), and 2(d), the bubble pairs travel in the direction of the smaller bubble and, in Figs. 2(c), 2(e), and 2(f), toward the bigger bubble. Clearly this effect also results from the presence of viscous forces, which break down conservatism of the system and cause skewness in it. A detailed mechanism of this phenomenon (which is, strictly speaking, not in the scope of this paper) is not quite understood yet and will be investigated elsewhere.

## IV. CONCLUSION

In this paper, a model has been proposed that makes it possible to calculate radial and translational motions of two interacting spherical gas bubbles in a strong acoustic field. The model allows for the radiation coupling between the bubbles up to terms of third order in the inverse separation distance, viscous drag forces on the bubbles, and effects of liquid compressibility on their volume pulsations. Using this model, numerical investigation of translational motion of two small, driven well below resonance, bubbles in sound fields with pressure amplitudes exceeding 1 bar has been made. It has been shown that for most combinations of bubble radii characteristic of acoustic streamers, a mutual approach results in a dynamical steady state at which the distance between the bubbles remains, on average, constant. It is supposed that this result can provide an explanation for the structure of acoustic streamers.

## ACKNOWLEDGMENT

This research was supported by the European Commission under the INCO Copernicus program.

[1] V. F. K. Bjerknes, *Fields of Force* (Columbia University Press, New York, 1906).

[2] Yu. A. Kobelev, L. A. Ostrovskii, and A. M. Sutin, Pis'ma Zh. Éksp. Teor. Fiz. **30**, 423 (1979).

[3] P. L. Marston, E. H. Trinh, J. Depew, and J. Asaki, in *Bubble Dynamics and Interface Phenomena*, edited by J. R. Blake *et al.* (Kluwer Academic, Dordrecht, 1994), pp. 343–353.

[4] I. Akhatov, U. Parlitz, and W. Lauterborn, J. Acoust. Soc. Am.

**96**, 3627 (1994); Phys. Rev. E **54**, 4990 (1996); W. Lauterborn and C. D. Ohl, Ultrason. Sonochem. **4**, 65 (1997).

[5] E. A. Zabolotskaya, Akust. Zh. **30**, 618 (1984) [Sov. Phys. Acoust. **30**, 365 (1984)]; A. A. Doinikov and S. T. Zavtrak, Phys. Fluids **7**, 1923 (1995); J. Acoust. Soc. Am. **99**, 3849 (1996).

[6] R. Mettin, I. Akhatov, U. Parlitz, C. D. Ohl, and W. Lauterborn, Phys. Rev. E **56**, 2924 (1997).

[7] J. B. Keller and M. Miksis, J. Acoust. Soc. Am. **68**, 628 (1980).

[8] E. W. Hobson, *The Theory of Spherical and Ellipsoidal Harmonics* (Cambridge University Press, London, 1931).

[9] B. V. Levich, *Physicochemical Hydrodynamics* (Prentice-Hall, Englewood Cliffs, NJ, 1962).